Spring 3-2009

Colocalization of increased transforming growth factor-β-induced protein (TGFBIp) and Clusterin in Fuchs endothelial corneal dystrophy

Ula V. Jurkunas

Maya Bitar
Marshall University, bitar@marshall.edu

Ian Rawe

Recommended Citation

Jurkunas UV, Bitar M, Rawe I. Colocalization of increased transforming growth factor-β-induced protein (TGFBIp) and Clusterin in Fuchs endothelial corneal dystrophy. Investigative Ophthalmology & Visual Science. 2009;50:1129-1136. https://dx.doi.org/10.1167/iovs.08-2525

Colocalization of Increased Transforming Growth Factor-β–Induced Protein (TGFBIp) and Clusterin in Fuchs Endothelial Corneal Dystrophy

Ula V. Jurkunas,[1,2,3] *Maya Bitar,*[2,3] *and Ian Rawe*[2]

Purpose. To investigate the differential expression of TGFBIp in normal human and Fuchs endothelial corneal dystrophy (FECD) endothelial cell–Descemet's membrane (HCEC-DM) complex, and to asses the structural role of TGFBIp and clusterin (CLU) in guttae formation.

Methods. HCEC-DM complex was dissected from stroma in normal and FECD samples. Proteins were separated by 2-D gel electrophoresis and subjected to proteomic analysis. N-terminal processing of TGFBIp was detected by Western blot analysis with two separate antibodies against the N- and C-terminal regions of TGFBIp. Expression of *TGFBI* mRNA was compared by using real-time PCR. Subcellular localization of TGFBIp and CLU in corneal guttae was assessed by fluorescence confocal microscopy.

Results. A major 68-kDa fragment and a minor 39-kDa fragment of TGFBIp were identified on 2-D gels. Western blot analysis revealed an age-dependent proteolytic processing of the TGFBIp N terminus resulting in the increased formation of 57-kDa ($P = 0.04$) and 39-kDa ($P = 0.03$) fragments in older donors. FECD HCEC-DM showed a significant increase in the 68-kDa ($P = 0.04$), 57-kDa ($P = 0.01$), and 39- kDa ($P = 0.03$) fragments of TGFBIp. Real-time PCR analysis revealed that *TGFBI* mRNA was significantly increased ($P = 0.04$) in FECD samples. TGFBIp formed aggregates at the lower portions of guttae, next to Descemet's membrane, whereas CLU localized mostly on top of the TGFBIp-stained areas at the level of the endothelial cell nuclear plane.

Conclusions. The overexpression of proaggregative protein CLU, and proadhesive protein TGFBIp, have been colocalized in the guttae. Such findings provide us with a better understanding of the major contributors involved in the aberrant cell–extracellular matrix interactions seen in the guttae of patients with FECD. (*Invest Ophthalmol Vis Sci.* 2009;50: 1129–1136) DOI:10.1167/iovs.08-2525

Fuchs endothelial corneal dystrophy (FECD) is the most common endogenous corneal endotheliopathy, leading to progressive corneal edema, blindness, and eventual need for corneal transplantation to restore vision. In early stages, FECD is characterized by extracellular collagenous deposits that accumulate posterior to Descemet's membrane, thicken it, and cause the formation of mound-shaped aggregates, called "guttae." The characteristic pattern on specular microscopy showing dark areas in the endothelial mosaic is due to the displacement of the endothelium posterior to the plane of focus by these excrescences. In the later stages, the coalescence of the guttae occurs, and a progressive disruption of the endothelial mosaic causes cell thinning, stretching, enlargement, and loss of hexagonal shape.[1] Eventually, there is a compromise in the intact covering of the endothelial monolayer as endothelial cell loss progresses in an inversely proportional manner to guttae formation. The considerable strain on corneal endothelial cells situated at the apices of these excrescences causes the morphologic changes that lead to the loss of barrier function as well as cell apoptosis, which has been widely implicated in FECD.[2] Still, the exact composition of these outgrowths or guttae is currently not clear.

Studies from this laboratory have described the results of 2-D gel analysis of proteins extracted from human corneal endothelial cell-Descemet's membrane (HCEC-DM) complexes dissected from the corneas of normal donors and patients with FECD.[3,4] These studies showed that there is a marked overexpression of the proaggregative, chaperone-like protein clusterin in FECD.[3] The staining of FECD corneas with CLU antibodies revealed a clustering of endothelial cells around the guttae as well as CLU staining in the centers of the guttae, suggesting the presence of cell remnants in these areas. Studies have shown that under stressed conditions, CLU tends to cause cell aggregation and induce the formation of junctional contacts between cells.[5] The results of the 2-D gel analysis also demonstrated a marked overexpression of the cell adhesion molecule TGFBIp in the FECD-affected HCEC-DM complexes. TGFBIp was detected as a series of spots, migrating at ~38 kDa. The number and intensity of these spots was greater in FECD HCEC-DM as opposed to those in normal control subjects. The purpose of the present study is to investigate further the role of TGFBIp in the characteristic guttae formation and its relation to CLU.

TGFBI (transforming growth factor [TGF]-β induced) gene encodes the transforming growth factor-β–induced protein (TGFBIp), an extracellular matrix protein that mediates cell adhesion by interacting with collagens, fibronectin, and integrins, mainly $\alpha 3\beta 1$.[6–10] This protein has been identified by *TGFBI* gene induction with TGF-β in a human adenocarcinoma line.[11] Mutations in the *TGFBI* gene are responsible for several corneal stromal dystrophies, such as Lattice dystrophy type I, Reis-Bückler dystrophy, Thiel-Behnke corneal dystrophy, granular corneal dystrophy II (Avellino corneal dystrophy), and granular corneal dystrophy type I.[12–15] Depending on the dystrophy, the mutation in the *TGFBI* gene manifest as stromal amyloid and/or nonamyloid deposits in which *TGFBI* itself has been colocalized.[16] Analysis of the pathologic corneas taken from the stromal dystrophy patients has revealed that there are mutation-specific changes in the processing of the full-size protein as opposed to unaffected corneas.[16] In the present study, we used immunocytochemistry to localize the TGFBIp

From the [1]Massachusetts Eye and Ear Infirmary, Boston, Massachusetts; [2]Schepens Eye Research Institute, Boston, Massachusetts; and the [3]Department of Ophthalmology, Harvard Medical School, Boston, Massachusetts.

Supported by National Eye Institute Grant K12 EY016335 (UVJ) and by Massachusetts Eye and Ear Lions Fund (UVJ).

Submitted for publication July 3, 2008; revised August 19 and October 6, 2008; accepted January 19, 2009.

Disclosure: **U.V. Jurkunas**, None; **M. Bitar**, None; **I. Rawe**, None

The publication costs of this article were defrayed in part by page charge payment. This article must therefore be marked "*advertisement*" in accordance with 18 U.S.C. §1734 solely to indicate this fact.

Corresponding author: Ula V. Jurkunas, Massachusetts Eye and Ear Infirmary, 243 Charles Street, Boston, MA 02114; ula_jurkunas@meei.harvard.edu.

deposition and to elucidate further the role of TGFBIp in guttae formation. Also, using antibodies against two nonoverlapping parts of the protein, we investigated whether there are changes in the processing of TGFBIp between FECD and normal endothelial samples. To obtain greater insight into the role of TGFBIp in the HCEC-DM complex, we also compared the TGFBIp expression patterns in the corneas of young and old normal donors.

Materials and Methods

Human Tissue

Donor confidentiality was maintained according to the Declaration of Helsinki. This study was approved by the Massachusetts Eye and Ear Institutional Review Board. Informed consent was obtained from patients undergoing corneal transplantation for FECD. After surgical removal of the FECD corneal buttons, two thirds of the button was used for the study, and one third was used for histopathologic confirmation of the diagnosis. Normal human corneal buttons were obtained from the Tissue Banks International (Baltimore, MD) and National Disease Research Interchange (Philadelphia, PA) and were used as normal control samples. The corneas were kept in storage medium for less than 72 hours before processing. We used our previously published criteria for obtaining normal control subjects from the tissue banks.[3,4]

Sample Preparation

Table 1 presents information regarding the normal and FECD tissue samples. Normal donors were decade-matched with FECD. Because of low protein or RNA content, two FECD samples contained two pooled corneas (Table 1, samples 8 and 15). Corneal buttons were recovered from storage medium (Optisol-GS; Bausch & Lomb Surgical, Irvine, CA) and briefly rinsed in PBS. Under a dissecting microscope, Descemet's membrane along with the endothelial cell layer (HCEC-DM complex) was dissected from the stroma and washed with 10 mM HEPES buffer (pH 7.4) before protein extraction. Samples used for 2-D gel electrophoresis were subjected to an additional washing step with HEPES buffer (10 mM, pH 7.4) to reduce the concentration of salts. Protein extraction buffer ER3 (Bio-Rad, Hercules, CA), containing 5 M urea, 2 M thiourea, 2% CHAPS, 2% SB 3-10, 40 mM Tris, 0.2% ampholyte (Bio-Lyte 3/10; Bio-Rad) ampholyte, and 1 mM tributyl phosphine (TBP), was added to the HCEC-DM sample. Proteins were solubilized by pipetting up and down to promote adequate mixing and then incubating the samples at room temperature for 30 minutes, followed by ultracentrifugation at 40,000 rpm, 21°C for 1 hour. HCEC-DM protein samples were used for 2-D gel electrophoresis and Western blot analysis. The protein concentration of the samples was determined by modified protein assay (Bio-Rad).

Table 1. Donor Information

Sample No.	FECD HCEC-DM Age	FECD HCEC-DM Sex	Normal HCEC-DM Age	Normal HCEC-DM Sex	Use of Samples
1			67	F	2-D gel
			64	M	
			59	M	
2			2	M	Western blot analysis
3			15	F	
4			18	M	
5			64	F	
6			72	F	
7			73	M	
8	69	M	67	F	Western blot analysis
	66	F	72	F	
9	75	F	73	M	
10	55	F	68	M	
11	78	F	73	M	
12	79	F	72	F	
13	69	F	68	F	Real-time PCR
14	59	M	69	M	
15	72	M	64	F	
	69	F			
16	64	F	65	F	Immunohistochemistry
17	87	F	71	M	

2-D Gel Electrophoresis and Protein Identification

For 2-D gel electrophoresis, the sample was prepared by pooling HCEC-DM protein extracts from five normal corneas of three donors (a 67-year-old woman, 64-year-old man, and 59-year-old man; Table 1, sample 1). Protein extract (150 μL) was loaded onto immobilized, pH 3 to 10 nonlinear gradient, 17 cm IPG strips (Bio-Rad) for passive rehydration for 14 hours of isoelectric focusing and second-dimensional separation were performed as previously reported.[3,4] Gels were then fixed in 10% methanol and 7% acetic acid, stained overnight with a protein gel stain (SYPRO Ruby; Invitrogen, Carlsbad, CA), and washed in water for 1 hour before imaging. Protein spots from the 2-D gel were imaged (ProEXPRESS Proteomic Imaging System; PerkinElmer, Boston, MA), using optimized excitation (480/80) and emission (650/150) filters for the protein gel stain. Gel plugs from the protein spots were excised by direct picking using a spot-picking robot equipped with a CCD camera (ProXcision; PerkinElmer) and filter sets for the red stain. Gel pieces were placed in a microtiter plate (ZipPlate; Millipore, Billerica, MA) and processed as described in the manufacturer's protocol. The identification of protein spots was performed by MALDI-TOF, as previously described.[3,4] Proteins were identified by searching a local copy of the NCBI protein database (National Center for Biotechnology Information, www.ncbi.nih.gov) using the ProFound search engine (Rockefeller University, New York, NY).

Western Blot Analysis

Age difference in TGFBIp expression by Western blot analysis was compared between three young (2, 15, and 18 years old) and three older (64, 68, and 73 years old) normal donors (Table 1, samples 2–7). TGFBIp expression was compared between five normal and FECD HCEC-DM samples (Table 1, samples 8–12). Equal amounts of protein were loaded on 10% bis-tris gels for SDS-PAGE. Peptides were then electrophoretically transferred to a polyvinylidene difluoride (PVDF) membrane (Millipore). Nonspecific binding was blocked by incubation for 1 hour at room temperature in 5% nonfat milk diluted in PBS. Membranes were incubated overnight at 4°C with rabbit polyclonal anti-TGFBIp (H-58; Santa Cruz Biotechnology, Santa Cruz, CA) diluted 1:100, goat polyclonal anti-TGFBIp (E-19; Santa Cruz Biotechnology) diluted 1:100, and mouse monoclonal anti-β-actin (Sigma-Aldrich, St. Louis, MO) diluted 1:6000 in blocking solution. The anti-TGFBIp antibodies were created against a recombinant TGFBIp (NCBI GI no. 2498193; National Center for Biotechnology Information, Bethesda, MD), and molecular weight ranges were confirmed by the affinity purification of the specific peptides by Santa Cruz Biotechnology. Blots were rinsed, reblocked, and exposed for 1 hour to horseradish peroxidase (HRP)–conjugated donkey anti-mouse IgG for β-actin, anti-rabbit IgG for clusterin, anti-rabbit IgG for TGFBIp (H-58), and anti-goat IgG for TGFBIp (E-19). All secondary antibodies were obtained from Jackson ImmunoResearch Laboratories, Inc. (West Grove, PA) and diluted 1:2000 in blocking solution. After washing in 0.1% Triton X-100, peptides were detected with a pico chemiluminescent substrate (SuperSignal; Pierce, Rockford, IL). Images were digitally scanned and analyzed with NIH Image software version 1.61 (developed by Wayne

Rasband, National Institutes of Health, Bethesda, MD; available at http://rsb.info.nih.gov/ij/index.html). Protein was normalized according to β-actin and total protein content. Experiments were repeated at least two times. Results were averaged and the standard deviation calculated. Statistical analysis by Student's unpaired *t*-test was performed (Excel 2002 for Windows XP; Excel, Redmond, WA). $P < 0.05$ was considered to be significant.

Real-Time PCR

Total RNA was extracted from normal and FECD HCEC-DM complexes (samples 13–15, Table 1) as recommended by the manufacturer (TRIzol; Invitrogen). Samples were purified from DNA contamination by treating them with amplification grade DNase I (Invitrogen). RNA quantity and quality were assessed by spectrophotometric analysis. For all samples, cDNA was prepared by reverse transcription with a commercially available kit (Promega, Madison, WI). Relative expression levels of *TGFBI* were assessed by real-time PCR with a sequence-detection system (ABI Prism model 7900 HT; Applied Biosystems Inc., [ABI] Foster City, CA). Primers and probes for *TGFBI* (*Taq*Man Gene Expression Assays; Invitrogen) and for the endogenous control β_2-microglobulin (β_2-MG; human B2M endogenous control, FAM/MGB probe, *Taq*Man Endogenous Controls) were obtained from ABI. Samples ($n = 3$) were assayed in duplicate in a total volume of 50 μL, using thermal cycling conditions of 2 minutes at 50°C and 10 minutes at 95°C followed by 50 cycles of 95°C for 15 seconds and 60°C for 1 minute. No-template controls were run in each assay to confirm lack of contamination in reagents used for amplification. For data analysis, the comparative threshold cycle (C_T) method was adopted with the relative mRNA levels in normal subjects selected as the calibrator. The C_T was set in the exponential phase of the amplification plot. To normalize the amount of target gene in each sample, the change in C_T (ΔC_T) was calculated by subtracting the average C_T of the endogenous control from that of the target gene. The amount of *TGFBI* mRNA in FECD was expressed relative to the amount present in the calibrator, using the formula $2^{-\Delta\Delta CT}$. Results were averaged, and the SEM was calculated. Statistical analysis with Student's unpaired *t*-test was performed (Excel 2002 for Windows XP; Microsoft). $P < 0.05$ was considered to be significant.

Immunocytochemical Localization of TGFBIp and Clusterin

Normal and FECD corneas (Table 1, samples 16 and 17) were washed in PBS and then fixed with 100% methanol for 10 minutes at −20°C. All subsequent steps were performed at room temperature. Corneas were washed in PBS, then permeabilized for 10 minutes with 1% Triton X-100 in PBS. Nonspecific binding was blocked using 4% bovine serum albumin (BSA; Fisher Scientific, Pittsburgh, PA) in PBS for 10 minutes. Corneas were incubated for 2 hours in rabbit polyclonal anti-clusterin (Santa Cruz Biotechnology), diluted 1:50 in 4% BSA in PBS, and goat polyclonal anti-TGFBIp (Santa Cruz Biotechnology), diluted 1:50 in 4% BSA in PBS. Corneas were washed three times in PBS for 10 minutes each and then incubated for 1 hour with fluorescein (FITC)-conjugated donkey anti-goat IgG (Jackson ImmunoResearch, West Grove, PA) diluted 1:200 in 4% BSA in PBS, rhodamine-conjugated donkey anti-rabbit IgG (Jackson ImmunoResearch). Nuclear stain was performed (TO-PRO-3; Invitrogen-Molecular Probes, Eugene, OR) diluted 1:2000 in PBS. Negative controls consisted of secondary antibody alone. After they were washed in PBS, the corneas were placed endothelial side up on slides in mounting medium (Vector Laboratories, Burlingame, CA). Digital images were obtained by confocal microscope (TSC-SP2; Leica, Bannockburn, IL). A *z*-series through the tissue was captured with a step size of 0.2 μm per image. Images were created by using a single series or by collapsing *z*-series images onto a single-image plane by projecting the maximum pixel intensity of the images.

Results

Analysis of TGFBIp Isoform Expression in Normal HCEC-DM Complex

Our previous studies comparing the proteome of FECD and normal corneal endothelium revealed a marked overexpression of TGFBIp in 2-D gels of FECD samples. In this study, we further investigated TGFBIp expression and proteolytic processing in normal human corneal endothelium. To characterize TGFBIp expression, we pooled HCEC-DM protein extracts from three normal donors and then subjected them to 2-D gel electrophoresis followed by MALDI-TOF analysis. MALDI-TOF identified TGFBIp in two areas of the gel. TGFBIp was identified as a series of spots with different pI migrating at two different relative molecular weights. The first row of spots identified as TGFBIp was located at the 68-kDa range within pI 3.0 to 8.0, as shown in brackets in Figure 1A. The major 68-kDa TGFBIp fraction constituted a series of spots that most likely represent different posttranslational modifications of TGFBIp. The second series of spots identified as TGFBIp was at 39-kDa range as shown in the lower brackets in Figure 1A. The 39-kDa fragment was formed by six spots within pI 4.5 to 6.0, apparently representing different posttranslational modification of this TGFBIp form as well. The analysis of the remainder of the spots on the 2-D gel did not reveal any additional TGFBIp forms.

TGFBIp processing was studied by Western blot analysis with antibodies reactive to two nonoverlapping parts of the TGFBIp. Figure 1B depicts the diagram of anti-TGFBIp 120-170 (E-19) and anti-TGFBIp 626-683 (H-58) binding sites (molecular weight range as provided by direct communication with Santa Cruz Biotechnology, 2008). Immunostaining of 1-D gels with anti-TGFBIp 120-170 and anti-TGFBIp 626-683 antibodies re-

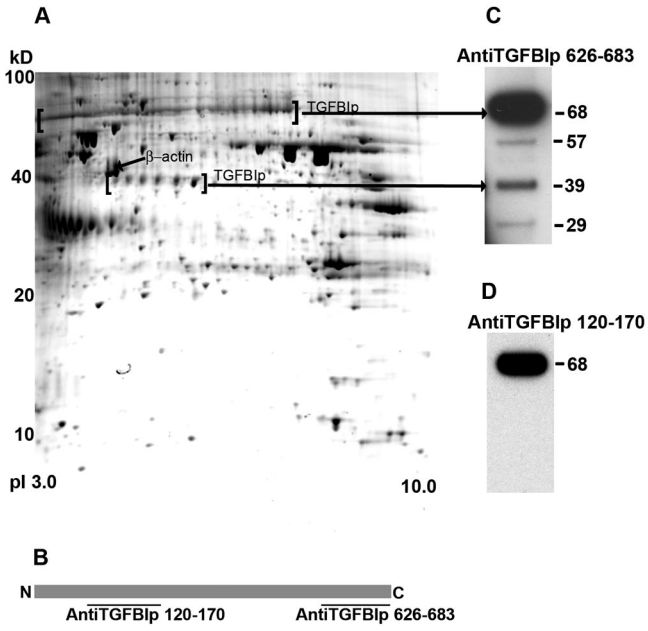

Figure 1. TGFBIp expression in normal human HCEC-DM. Two-dimensional gel of HCEC-DM proteins pooled from five corneas of three normal donors (**A**). The group of TGFBIp spots in the range of 68 and 39 kDa are indicated within brackets. *Arrow*: position of β-actin. The diagram of anti-TGFBIp 120-170 and 626-683 antibody binding is presented in a diagram (**B**). Western blot analysis of HCEC-DM protein extracts resolved on 1-D gels with anti-TGFBIp 626-683 antibody (**C**) and anti-TGFBIp 120-170 antibody (**D**). *Long arrows*: alignment of 68- and 39-kDa TGFBIp fragments resolved on a 2-D gel and a Western blot.

vealed a major band migrating at 68 kDa, which corresponded to the full-size protein seen on the 2-D gel (Figs. 1C, 1D). The anti-TGFBIp 626-683, which reacts with the C terminus of TGFBIp, revealed several minor species of TGFBIp. The molecular weights of the TGFBIp fragments found on the blots were very similar to the previously published molecular weights of TGFBIp fragments found in the protein extracts of the whole corneas.[16] Apart from the 68-kDa protein, anti-TGFBIp 626-683 recognized fragments of 57, 39, and 29 kDa. The 39-kDa fragment corresponded to relative molecular weight of the minor TGFBIp species seen on the 2-D gel. In contrast, anti-TGFBIp 120-170 which specifically reacts with the N terminus of TGFBIp, did not detect these minor TGFBIp species. This differential staining suggests that minor TGFBIp species not detected with the antibody against the N terminus represent N-terminal deletions during the processing of the full-size protein.

Analysis of Age-Related Differences

To explore the age-related differences in TGFBIp expression, six normal corneas at different ages were analyzed with the Western blot analysis (Table 1, samples 2–7). The immunostaining with anti-TGFBIp 626-683 antibody to the C terminus revealed a different staining pattern at different donor ages. Figure 2A shows a representative blot of 2-, 15-, 64-, and 73-year-old donors, Figure 2B presents the densitometric comparison of all six samples based on normalization to β-actin, and Figure 2C presents the densitometric comparison of all six samples based on normalization to total protein amount. The comparison of protein levels between young and old donors revealed similar results when TGFBIp content was normalized to β-actin or to total protein amount. The major band at 68-kDa range was present in all ages. The 57-kDa band was present only in older donors ($P = 0.04$), indicating that this fragment of TGFBIp is formed due to age-related proteolytic processing. On average, there was a twofold increase in the 39-kDa band in older individuals ($P = 0.03$). The 29-kDa band was also present only in older donors, but it showed variable intensity between the specimens rendering it not statistically significantly elevated in older HCEC-DM complexes ($P = 0.05$) when TGFBIp content was normalized to β-actin, but was significantly elevated in older samples ($P = 0.01$) when TGFBIp content was normalized to total protein content.

Differential Expression of TGFBIp Forms in Normal and FECD Endothelium

Prior proteomic studies revealed a significant overexpression of TGFBIp in FECD samples on 2-D gels.[3] To investigate further the differential expression of TGFBIp forms in FECD and normal HCEC-DM samples, Western blot analysis was performed with antibodies against N and C termini of TGFBIp. The Western blot data obtained from one pair of pooled samples (Table 1, sample 8) and four pairs of nonpooled samples (Table 1, samples 9–12) was identical. Figure 3 shows a representative blot with anti-TGFBIp for the C terminus (Fig. 3A) and a representative blot with anti-TGFBIp for N terminus (Fig. 3B), and Figure 3C presents the densitometric comparison. There was a marked overexpression of most TGFBIp forms in FECD specimens as opposed to normal subjects. On average, there was a fivefold increase in the full-size protein (68-kDa band) in FECD ($P = 0.04$), as well as statistically significant increase in minor TGFBIp species: the 57-kDa band ($P = 0.01$) and 39-kDa band ($P = 0.03$) seen in FECD. The 29-kDa TGFBIp band was increased in FECD endothelium but not at a statistically significant level ($P = 0.11$). To compare protein levels between FECD and normal specimens, results were normalized to β-actin. The third column in the blots shows a normal specimen

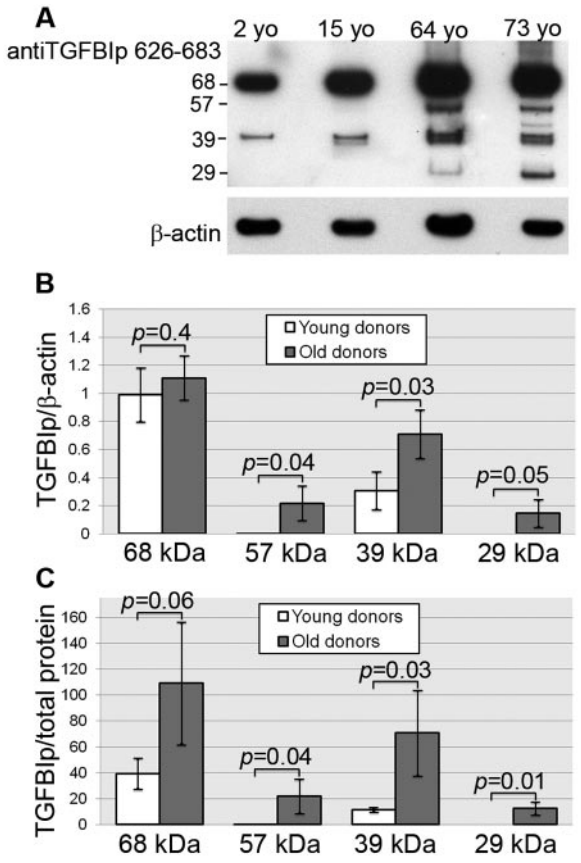

FIGURE 2. Age-related TGFBIp expression pattern. Representative Western blot analysis comparing anti-TGFBIp 626-683 expression of HCEC-DM extracts from normal 2-, 15-, 64-, and 73-year-old donors (**A**). β-Actin was used for normalization of protein loading. (**B**, **C**) Densitometric comparison of the average expression of TGFBIp fragments (Table 1, samples 2–7). Bars, SD.

loaded at a protein concentration twice as high as that in the first two columns (Figs. 3A, 3B). Such higher loading was performed to illustrate that both FECD and normal samples generally exhibited the same TGFBIp species but at higher levels in FECD when loading was normalized with β-actin. The 29-kDa band had variable and faint presence in most normal samples. The single band (68-kDa) that stained with anti-TGFBIp 120-170 antibody was also markedly increased in FECD, corroborating that the full-size TGFBIp is overexpressed in FECD. No other bands were detected with this antibody to the N terminus. FECD specimens demonstrated an increase in levels of all these fragments but did not reveal any new or unusual forms of TGFBIp.

Real-Time PCR Comparing *TGFBI* Expression between Normal and FECD HCEC-DM

Proteomic analysis and Western blot data revealed the upregulation of TGFBIp expression in FECD-affected corneal endothelium. To investigate this difference, real-time PCR was performed to evaluate the mRNA level of *TGFBI*. The PCR analysis was performed by using previously optimized primers and probes from ABI. Three different samples (samples 13–15) were used to compare the *TGFBI* mRNA expression between FECD and normal control subjects. The real-time PCR showed an upregulation of *TGFBI* mRNA levels in FECD samples when normalized with the internal control, β2-MG (Fig. 4). The mean ± SEM relative expression of *TGFBI* mRNA in the FECD

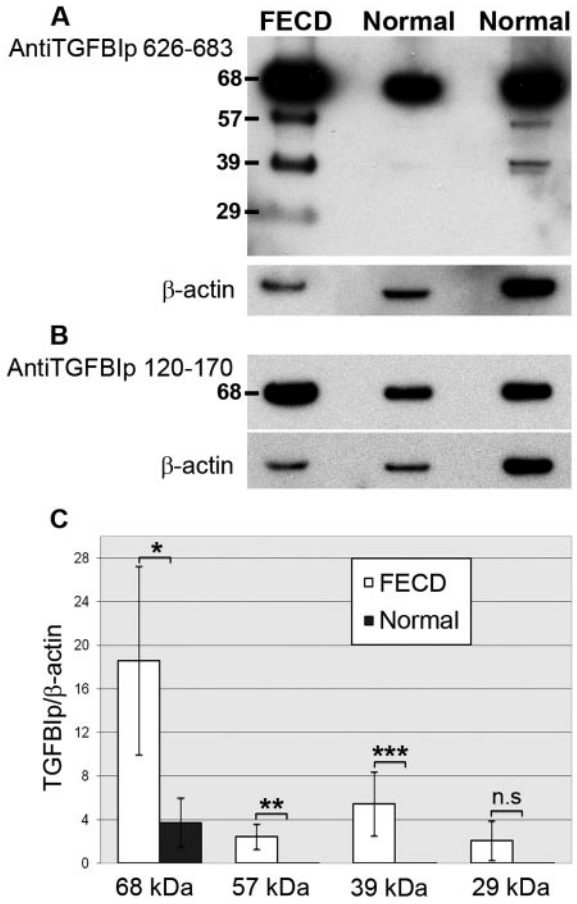

FIGURE 3. Comparison of TGFBIp expression patterns between FECD and normal HCEC-DM. Representative Western blot analysis of anti-TGFBIp 626-683 (**A**) and anti-TGFBIp 120-170 (**B**) comparing TGFBIp expression in FECD and normal HCEC-DM (Table 1, sample 12). The same normal sample was used in the second and third columns but with twice as high loading in the third column. β-Actin was used for normalization of protein loading. (**C**) Densitometric comparison of the average expression of TGFBIp fragments based on the anti-TGFBIp 626-683 results. Bars, SD. $^{*}P = 0.04$; $^{**}P = 0.01$; $^{***}P = 0.03$; NS, not statistically significant.

group (2.35 ± 0.23) was significantly higher than that in normal subjects (1.31 ± 0.38; $P = 0.04$).

Colocalization of TGFBIp and Clusterin in FECD

Previous immunofluorescence studies showed a characteristic CLU staining pattern in FECD endothelium with a rosette-type clustering of endothelial cells around dark centers representing corneal guttae. Indirect immunofluorescence analysis was performed to investigate the relationship between TGFBIp and CLU and to compare their localization in the endothelium of normal and FECD donors. Figure 5 presents confocal images in which the *z*-series was collapsed onto a single-image plane. Figures 5A–D present confocal images of normal endothelium. In normal tissue, a relatively uniform, punctate distribution of TGFBIp and CLU was observed within the cytoplasm (Figs. 5A, 5B). Descemet's membrane revealed bright fluorescence with anti-TGFBIp antibody in all the specimens (data not shown). Of note, the TGFBIp staining pattern in FECD endothelium (Figs. 5E–H) was different from that of normal HCECs. The dark areas which did not contain the nuclei and were considered to be corneal guttae had significant staining with both TGFBIp and CLU in FECD samples (Figs. 5E–H, asterisks). In the centers of guttae, TGFBIp colocalized with CLU most of the time (Figs. 5E, 5F, 5H, arrows). FECD tissue showed a much lower cell density than normal tissue; diffuse but less bright TGFBIp staining was visible even outside defined guttae, indicating the staining of the Descemet's membrane in areas devoid of cells. Negative control experiments consisted of normal corneas incubated with secondary antibody only and no TGFBIp or CLU-positive staining of either cells or Descemet's membrane was observed under these conditions, indicating the specificity of primary antibody staining (Figs. 5I–J).

To explore further the relationship between CLU and TGFBIp staining single *z*-plane images were taken through the guttae of FECD tissue at various depths (Fig. 6). A representative image through the apical part of endothelium at the level of the nuclear plane showed intense intracellular, intranuclear, and extracellular staining with CLU (Figs. 6B, 6D). The extracellular staining was most abundant in the center of the depicted gutta. At this particular plane, there was only faint staining in the center of the gutta with anti-TGFBIp antibody (Fig. 6A). Figures 6E–H represents the images that were taken 1.0 μm deeper into the cornea. At this plane, both TGFBIp and CLU staining colocalized in the center of the gutta. Figures 6I–L represents the images that were taken 3.8 μm deeper into the cornea beyond the nuclear plane of the same gutta. At this plane, the center of the gutta had bright staining with anti-TGFBIp antibody. The images taken at an even deeper level showed significant TGFBIp staining at the level of Descemet's membrane (data not shown). Overall, the images manifested specific colocalization of TGFBIp with CLU in the centers of corneal guttae of FECD specimens. TGFBIp tended to localize to the lower portions of guttae next to Descemet's membrane and CLU localized on top of the TGFBIp-stained areas.

DISCUSSION

The TGF-β-induced protein is mainly an extracellular matrix protein that has a secretory signal sequence at the N terminus, four homologous internal domains, and a cell-attachment site (consisting of RGD amino acids) at the C terminus.[6] The main function of TGFBIp is attributed to its ability to bind various ligands and mediate cell adhesion via the RGD sequence.[7] In our previous studies, we detected a marked overexpression of clusterin and TGFBIp in FECD endothelium.[3] In the present study, we performed a targeted analysis of TGFBIp processing in normal and FECD HCEC-DM and compared TGFBIp expression in young and old donors. The colocalization of TGFBIp and CLU expression in guttae provided us with an insight into the structural composition of these extracellular excrescences.

Proteomic analysis of normal HCEC-DM showed that TGFBIp is abundantly expressed in the endothelial-DM complex. TGFBIp has multiple threonine, tyrosine, and serine sites which allow phosphorylation and thus posttranslational modification.[16] On 2-D gels, 68- and 39-kDa TGFBIp fragments migrated as series of spots with different pIs, most likely representing different

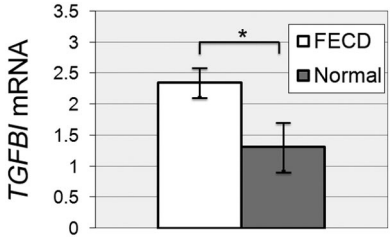

FIGURE 4. Comparison of *TGFBI* gene expression between FECD and normal HCEC-DM by real-time PCR. Mean relative expression of mRNA in normal subjects and in patients with FECD. Bars, SEM. $^{*}P = 0.04$.

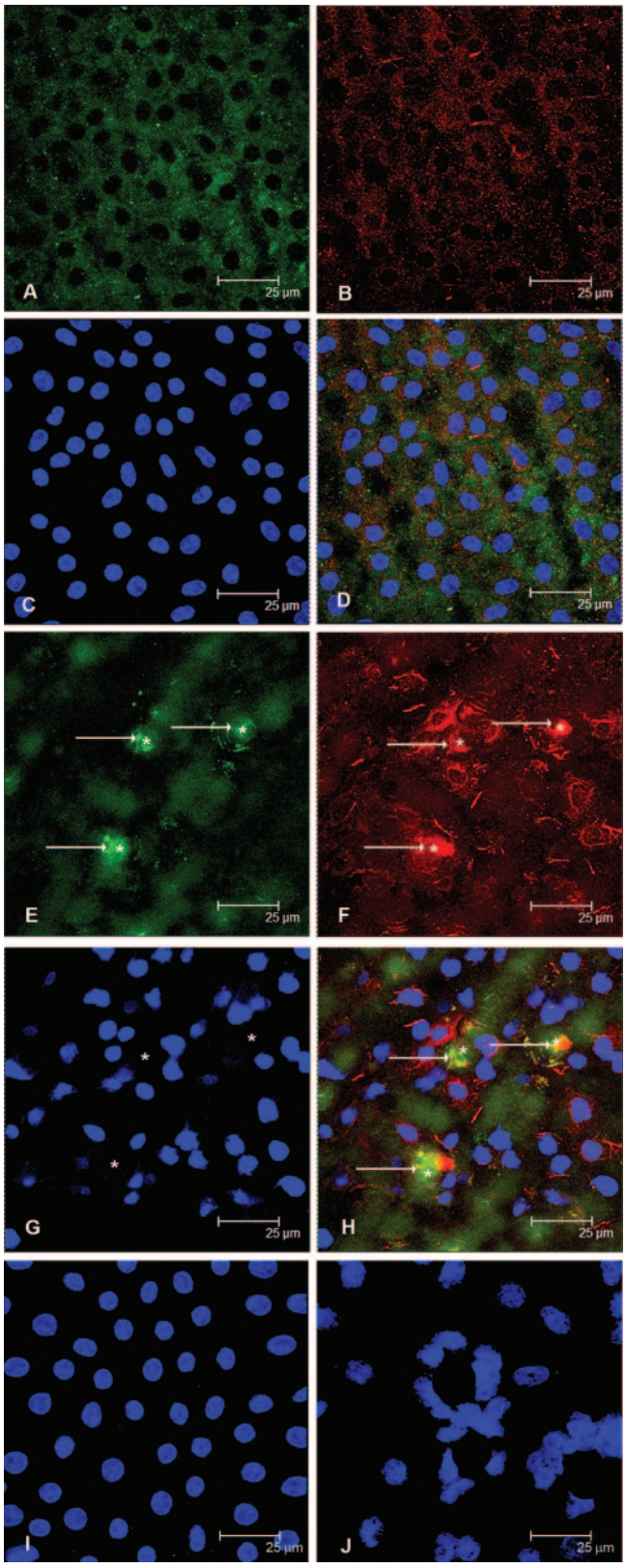

FIGURE 5. Colocalization of TGFBIp and CLU in normal and FECD corneal endothelium. Representative confocal images of normal (**A–D**) and FECD (**E–H**) endothelium in wholemounts of corneal tissue. Uniform TGFBIp staining (*green*) and CLU staining (*red*) was present in the cytoplasm of normal corneal endothelium (**A**, **B**). (**C**) Staining of nuclei (*blue*); (**D**) an overlay of the three images. (**E–H**, ✶) The guttae that did not contain the nuclear stain. (**E**) TGFBIp staining (*arrows*) in FECD-affected cells with increased brightness in the areas of guttae (✶). (**F**) CLU staining (*arrows*) in the same tissue which colocalized to the TGFBIp-stained areas in the centers of guttae (✶). (**G**) Stained nuclei in the same tissue with nuclei surrounding guttae (✶); (**H**) overlay of the three images colocalizing TGFBIp and CLU (*arrows*). Negative control, incubated in secondary antibodies, shows no discernible staining for TGFBIp and CLU in normal (**I**) and FECD (**J**) samples. Final magnification, 400× with 3 zoom.

posttranslational modifications of TGFBIp. This finding is in agreement with the other studies in which 2-D electrophoresis was performed on the whole corneal extracts and identified TGFBIp in multiple spots migrating at the same molecular weight, but with different pIs.[16] The fact that the 57- and 29-kDa fragments were repeatedly identified by Western blot but not on the 2-D gels is most likely because these forms are present in much lower concentrations and because MALDI-TOF is not sensitive enough to identify them.

The analysis of TGFBIp content using antibodies against two nonoverlapping parts of the protein revealed the presence of C-terminal fragments of the protein that varied in relative concentration with increasing age of the donors. In addition to the major 68-kDa band corresponding to the full-size protein, we identified a set of fragments that are most likely the proteolysis products characteristic for TGFBIp turnover in normal HCEC-DM. It is possible that the TGFBIp fragments were created from degradation by extracellular proteases. Nevertheless, a more plausible explanation is the fragment formation from normal TGFBIp turnover in corneal endothelium, since almost identical molecular weight fragments were detected in the study by Korvatksa et al.,[16] in which N-terminal sequencing and immunostaining were performed to characterize TGFBIp content in the whole corneas. Our study showed an increase in the levels of the 39-kDa fragment with increasing age of donors. Of note, only 68- and 39-kDa bands were present throughout the age range of donors. The other fragments (57- and 29-kDa) appeared to be present in older age samples only, implicating the age-related differences in normal TGFBIp turnover. The gradual thickening of Descemet's membrane and building of the posterior nonbanded layer with age is in agreement with the increasing accumulation of TGFBIp which is known to have a physiological interaction with collagens.[7,17,18] Previous studies performed on whole rabbit corneal buttons showed an increase in steady state levels of *TGFBI* mRNA that correlated with an increasing rate of collagen accumulation during corneal morphogenesis.[18] Several immunohistochemical studies have localized TGFBIp in normal Descemet's membrane, posterior collagenous layer, and retrocorneal fibrous membrane, inferring its role as a structural element of the aging and injured Descemet's membrane.[19–22] The exact role of TGFBIp is not known, but its abundance in the extracellular milieu of endothelium implies a substantial role in the cell–Descemet's membrane interaction.

A study comparing 2-D gels of FECD and normal donors revealed an increase in TGFBIp spot intensity and number in FECD samples.[3] To analyze this difference further, we performed Western blot analysis comparing TGFBIp expression in normal and FECD HCEC-DM samples. Expression of 68-, 57-, and 39-kDa fragments was statistically significantly higher in the FECD HCEC-DM. The expression of the 29-kDa fragment was elevated in FECD but not at a significant level. To corroborate the increase of TGFBIp levels in FECD, we compared its expression at the gene level between normal and FECD samples. The finding that levels of *TGFBI* mRNA were significantly increased in FECD samples further substantiates the proteomic data and indicates that the source of the differences stem from increased gene transcription.

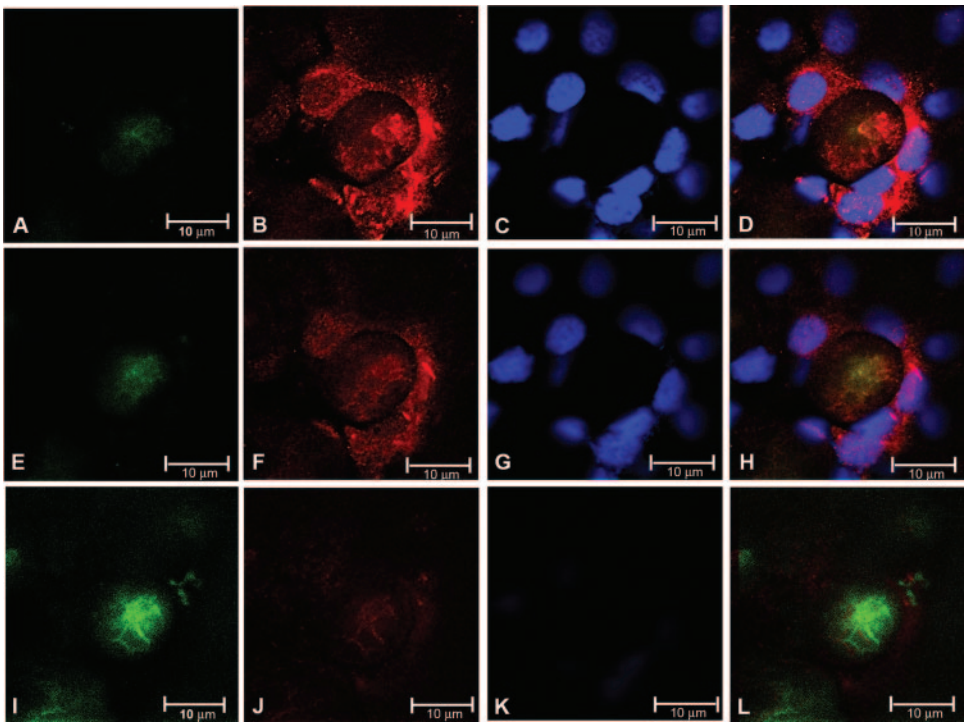

FIGURE 6. Localization of TGFBIp and CLU in the gutta. Representative confocal images taken through a single, 0.2-μm-thick z-plane of a gutta at the level of the endothelial nuclear plane (**A–D**), 1.0 μm (**E–H**), and 3.8 μm (**I–L**) deeper toward the Descemet's membrane. Images were taken after immunostaining for TGFBIp (*green*) (**A**, **E**, **I**) and CLU (*red*) (**B**, **F**, **J**) and nuclear staining (*blue*) (**C**, **G**, **K**). (**D**, **H**, **L**) Overlay of the three images. Final magnification, 400× with 8 zoom.

Studies analyzing pathologic stromal deposits due to mutation in the *TGFBI* gene have also identified an accumulation of TGFBIp fragments in dystrophic corneas compared with normal ones.[16,23,24] TGFBIp has been shown to colocalize and coaggregate into these deposits, which were composed of either amyloid or nonamyloid depending on the form of stromal dystrophy.[16] In addition to the increase in TGFBIp production, the analysis of these corneas detected overexpression of aberrant forms of TGFBIp that varied in their molecular weight depending on the type of dystrophy. In our study of FECD samples, we did not detect any aberrant or unusual forms of TGFBIp that were not present in normal age-matched control subjects, implying that probably there is no intrinsic mutation in the *TGFBI* gene causing the accumulation of the protein. This is in contrast to the findings in the stromal dystrophies where overexpression of both normal and aberrant forms of TGFBIp has been attributed to the *TGFBI* gene mutations.[16]

The immunohistologic analysis revealed an interesting pattern of CLU and TGFBIp colocalization in the guttae, the excrescences characteristic of Fuchs corneal dystrophy. The staining for TGFBIp was prominent throughout Descemet's membrane and showed a marked increase in intensity at the centers of the guttae. CLU was also present in the centers of the guttae but on top of TGFBIp staining, closer to the apical side of the endothelium. The diagram in Figure 7 shows a schematic representation of the relationship of CLU and TGFBIp role in guttae formation. This is the first known study to colocalize CLU and TGFBIp in these pathologic extracellular matrix deposits. There is no known correlation in the literature between clusterin and TGFBIp. It is known, though, that CLU overexpression at the times of cellular stress (including oxidative stress) causes the cells to aggregate via cell–cell and cell–substratum interactions.[5] The driving force of these interactions oftentimes is the production of cell adhesive molecules and junctional complexes. In a renal injury model, such interactions are capable of preserving the integrity of the renal epithelial barrier.[25,26] When the cell–matrix interactions are disrupted, a form of apoptosis called anoikis ensues. Similarly in FECD, there is an overproduction of the cell-adhesion mol-

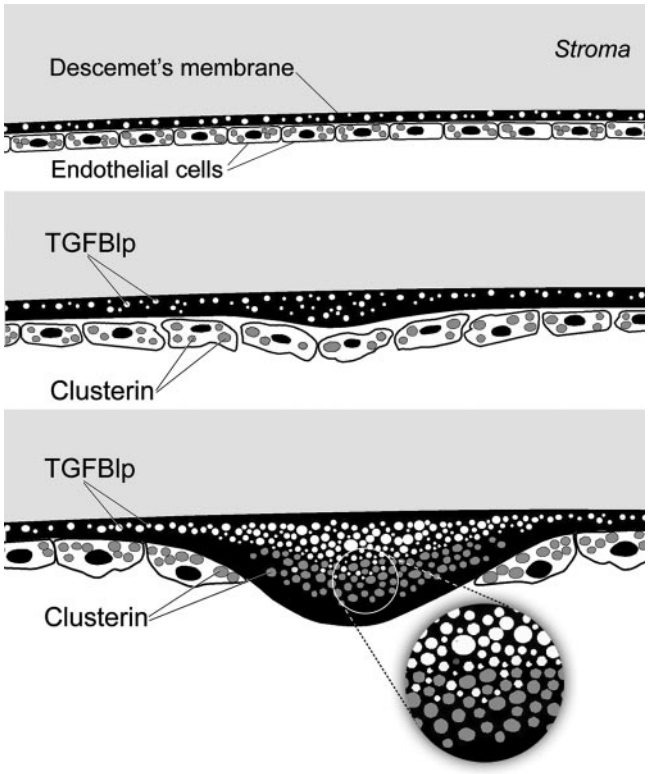

FIGURE 7. Schematic representation of the role TGFBIp and CLU in guttae formation. There is a gradually increasing production of TGFBIp and CLU in the centers of guttae. TGFBIp accumulates in close proximity to Descemet's membrane, whereas CLU forms aggregates on top of the TGFBIp deposits at the endothelial cell level. Both TGFBIp and CLU colocalized in the middle of the guttae (*inset*).

ecule, TGFBIp in the setting of the prolonged tissue injury and pathologic CLU overexpression. It is possible that the endothelial cells under stressors of the dystrophic degeneration are clumping via the action of CLU and are adhering to their substratum via the action of TGFBIp. The attempt of the cells to attach to their substratum is progressively disrupted during guttae formation, thus rendering the cells susceptible to apoptosis.

In conclusion, there is an increased production and modification of TGFBIp in the aging HCEC-DM complex. The increase in TGFBIp production is even greater in FECD compared with the age-matched normal control subjects. The proaggregative protein CLU and the proadhesive protein TGFBIp colocalize in the centers of guttae. Even though such findings cannot infer the functional role of these proteins in the pathogenesis of the dystrophy, it provides us with a better understanding of the major culprits involved in the aberrant cell–extracellular matrix interactions.

Acknowledgments

The authors thank all the Massachusetts Eye and Ear cornea surgeons and Peter Rapoza (Ophthalmic Consultants of Boston) for arranging the donation of the corneal specimens, Nancy C. Joyce (Schepens Eye Research Institute and The Department of Ophthalmology, Harvard Medical School) for critical reading of the manuscript, and Peter Mallen for assistance with the graphics.

References

1. Waring GO 3rd, Bourne WM, Edelhauser HF, Kenyon KR. The corneal endothelium: normal and pathologic structure and function. *Ophthalmology.* 1982;89:531–590.
2. Borderie VM, Baudrimont M, Vallee A, Ereau TL, Gray F, Laroche L. Corneal endothelial cell apoptosis in patients with Fuchs' dystrophy. *Invest Ophthalmol Vis Sci.* 2000;41:2501–2505.
3. Jurkunas UV, Bitar MS, Rawe I, Harris DL, Colby K, Joyce NC. Increased clusterin expression in Fuchs' endothelial dystrophy. *Invest Ophthalmol Vis Sci.* 2008;49:2946–2955.
4. Jurkunas UV, Rawe I, Bitar MS, et al. Decreased expression of peroxiredoxins in Fuchs' endothelial dystrophy. *Invest Ophthalmol Vis Sci.* 2008;49:2956–2963.
5. Schwochau GB, Nath KA, Rosenberg ME. Clusterin protects against oxidative stress in vitro through aggregative and nonaggregative properties. *Kidney Int.* 1998;53:1647–1653.
6. Runager K, Enghild JJ, Klintworth GK. Focus on molecules: transforming growth factor beta induced protein (TGFBIp). *Exp Eye Res.* 2008;87(4):298–9.
7. Hashimoto K, Noshiro M, Ohno S, et al. Characterization of a cartilage-derived 66-kDa protein (RGD-CAP/beta ig-h3) that binds to collagen. *Biochim Biophys Acta.* 1997;1355:303–314.
8. Billings PC, Whitbeck JC, Adams CS, et al. The transforming growth factor-beta-inducible matrix protein (beta)ig-h3 interacts with fibronectin. *J Biol Chem.* 2002;277:28003–28009.
9. LeBaron RG, Bezverkov KI, Zimber MP, Pavelec R, Skonier J, Purchio AF. Beta IG-H3, a novel secretory protein inducible by transforming growth factor-beta, is present in normal skin and promotes the adhesion and spreading of dermal fibroblasts in vitro. *J Invest Dermatol.* 1995;104:844–849.
10. Kim JE, Kim SJ, Lee BH, Park RW, Kim KS, Kim IS. Identification of motifs for cell adhesion within the repeated domains of transforming growth factor-beta-induced gene, betaig-h3. *J Biol Chem.* 2000; 275:30907–30915.
11. Skonier J, Neubauer M, Madisen L, Bennett K, Plowman GD, Purchio AF. cDNA cloning and sequence analysis of beta ig-h3, a novel gene induced in a human adenocarcinoma cell line after treatment with transforming growth factor-beta. *DNA Cell Biol.* 1992;11:511–522.
12. Munier FL, Korvatska E, Djemai A, et al. Kerato-epithelin mutations in four 5q31-linked corneal dystrophies. *Nat Genet.* 1997;15:247–251.
13. Zhao XC, Nakamura H, Subramanyam S, et al. Spontaneous and inheritable R555Q mutation in the TGFBI/BIGH3 gene in two unrelated families exhibiting Bowman's layer corneal dystrophy. *Ophthalmology.* 2007;114:e39–e46.
14. Okada M, Yamamoto S, Tsujikawa M, et al. Two distinct kerato-epithelin mutations in Reis-Bucklers corneal dystrophy. *Am J Ophthalmol.* 1998;126:535–542.
15. Yamamoto S, Okada M, Tsujikawa M, et al. The spectrum of beta ig-h3 gene mutations in Japanese patients with corneal dystrophy. *Cornea.* 2000;19:S21–S23.
16. Korvatska E, Henry H, Mashima Y, et al. Amyloid and non-amyloid forms of 5q31-linked corneal dystrophy resulting from kerato-epithelin mutations at Arg-124 are associated with abnormal turnover of the protein. *J Biol Chem.* 2000;275:11465–11469.
17. Rawe IM, Zhan Q, Burrows R, Bennett K, Cintron C. Beta-ig: molecular cloning and in situ hybridization in corneal tissues. *Invest Ophthalmol Vis Sci.* 1997;38:893–900.
18. El-Shabrawi Y, Kublin CL, Cintron C. mRNA levels of alpha1(VI) collagen, alpha1(XII) collagen, and beta ig in rabbit cornea during normal development and healing. *Invest Ophthalmol Vis Sci.* 1998;39:36–44.
19. Takacs L, Csutak A, Balazs E, Berta A. Immunohistochemical detection of betaIG-H3 in scarring human corneas. *Graefes Arch Clin Exp Ophthalmol.* 1999;237:529–534.
20. Leung EW, Rife L, Smith RE, Kay EP. Extracellular matrix components in retrocorneal fibrous membrane in comparison to corneal endothelium and Descemet's membrane. *Mol Vis.* 2000;6:15–23.
21. Hirano K, Klintworth GK, Zhan Q, Bennett K, Cintron C. Beta ig-h3 is synthesized by corneal epithelium and perhaps endothelium in Fuchs' dystrophic corneas. *Curr Eye Res.* 1996;15:965–972.
22. Akhtar S, Bron AJ, Hawksworth NR, Bonshek RE, Meek KM. Ultrastructural morphology and expression of proteoglycans, betaig-h3, tenascin-C, fibrillin-1, and fibronectin in bullous keratopathy. *Br J Ophthalmol.* 2001;85:720–731.
23. Streeten BW, Qi Y, Klintworth GK, Eagle RC Jr, Strauss JA, Bennett K. Immunolocalization of beta ig-h3 protein in 5q31-linked corneal dystrophies and normal corneas. *Arch Ophthalmol.* 1999;117:67–75.
24. Korvatska E, Munier FL, Chaubert P, et al. On the role of kerato-epithelin in the pathogenesis of 5q31-linked corneal dystrophies. *Invest Ophthalmol Vis Sci.* 1999;40:2213–2219.
25. Silkensen JR, Skubitz KM, Skubitz AP, et al. Clusterin promotes the aggregation and adhesion of renal porcine epithelial cells. *J Clin Invest.* 1995;96:2646–2653.
26. Tung PS, Burdzy K, Wong K, Fritz IB. Competition between cell-substratum interactions and cell-cell interactions. *J Cell Physiol.* 1992;152:410–421.